

Supporting Information

A simple and easy-to-prepare imidazole-based probe for the selective chromo-fluorogenic recognition of biothiols and of Cu(II) in HeLa Cells and in aqueous environments

Hazem Essam Okda,^{a,b,c} Sameh El Sayed,^{a,b,c} Ismael Otri,^{a,b,c} R. Cristina M. Ferreira,^d Susana P. G. Costa,^d M. Manuela M. Raposo,^{d*} Ramón Martínez-Máñez^{a,b,c*} and Félix Sancenón^{a,b,c}

^a Instituto Interuniversitario de Investigación de Reconocimiento Molecular y Desarrollo Tecnológico (IDM).
Universitat Politècnica de Valencia, Universitat de València, Camino de Vera s/n, 46022 Valencia, Spain

^b CIBER de Bioingeniería, Biomateriales y Nanomedicina (CIBER-BBN)

^c Departamento de Química, Universitat Politècnica de València, Camino de Vera s/n, 46022 Valencia, Spain

^d Centro de Química, Universidade do Minho, Campus de Gualtar, 4710-057, Braga, Portugal.

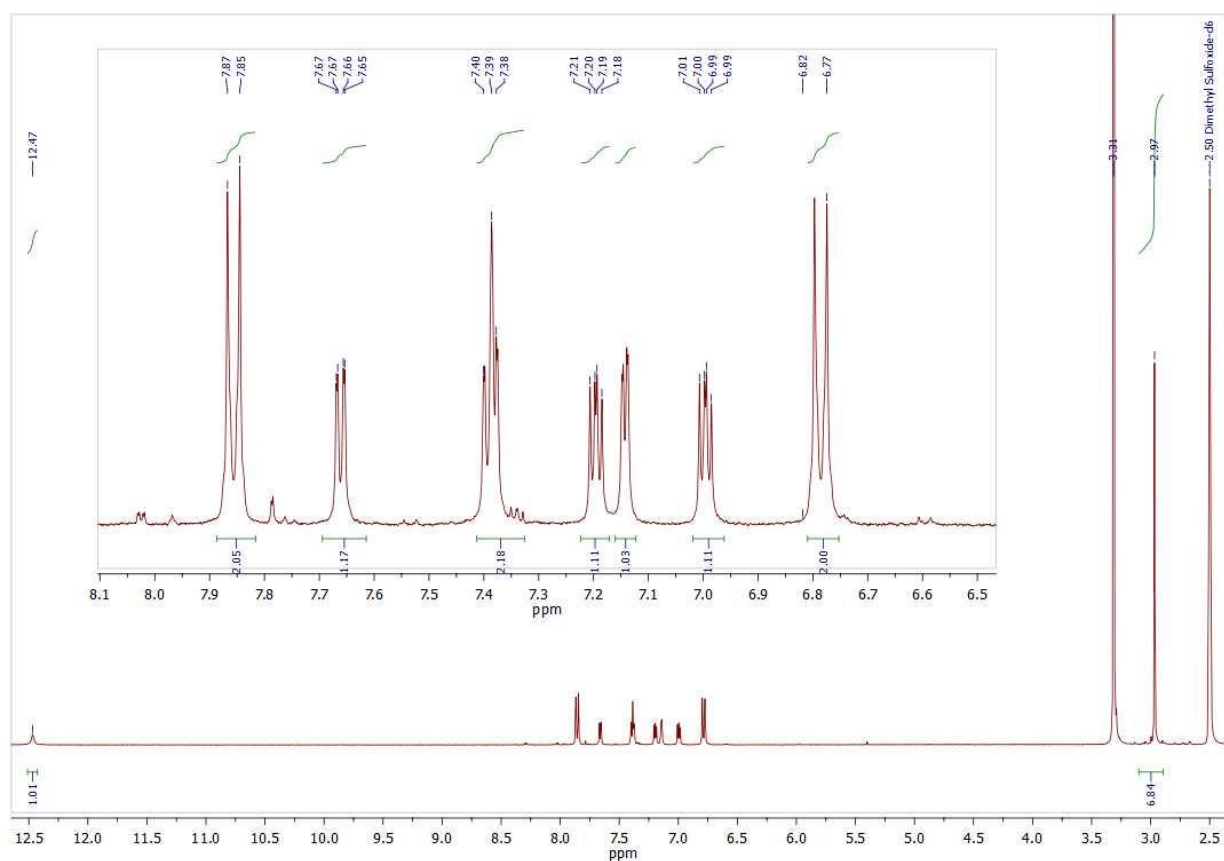


Figure S1. ¹H NMR spectra of probe 1 in DMSO-*d*₆.

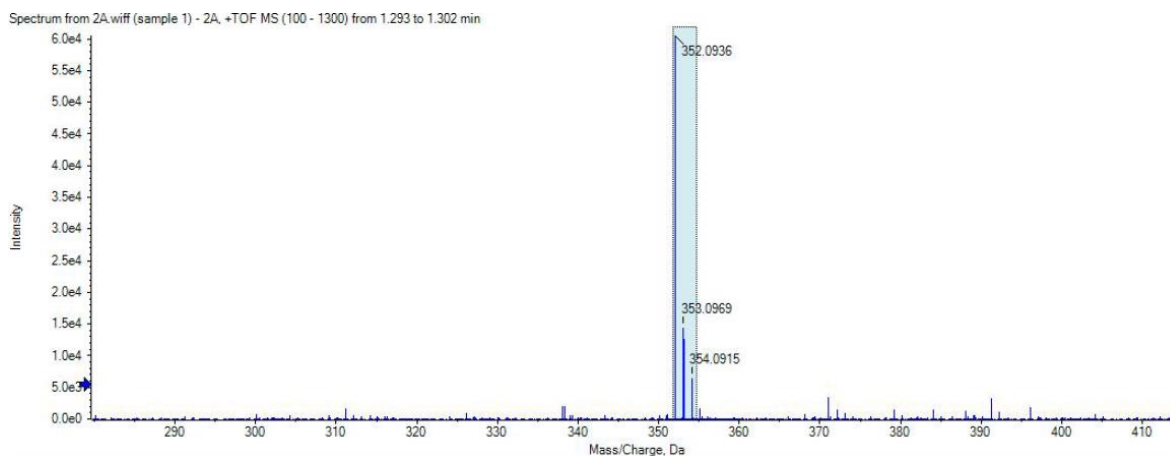


Figure S2. ESI-MS spectra of probe 1.



Figure S3. Colour changes observed in acetonitrile solutions of probe 1 (1.0×10^{-5} mol L⁻¹) upon addition of 10 equiv. of selected metal cations.

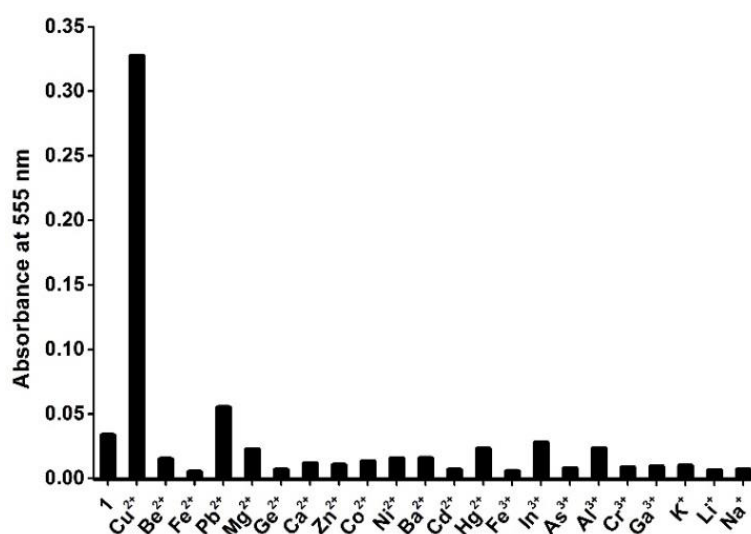


Figure S4. Absorbance at 555 nm of water (pH 7.4)-acetonitrile 90:10 v/v (1.0×10^{-5} mol L⁻¹) solutions of probe 1 alone and in the presence of selected metal cations (10 eq.).

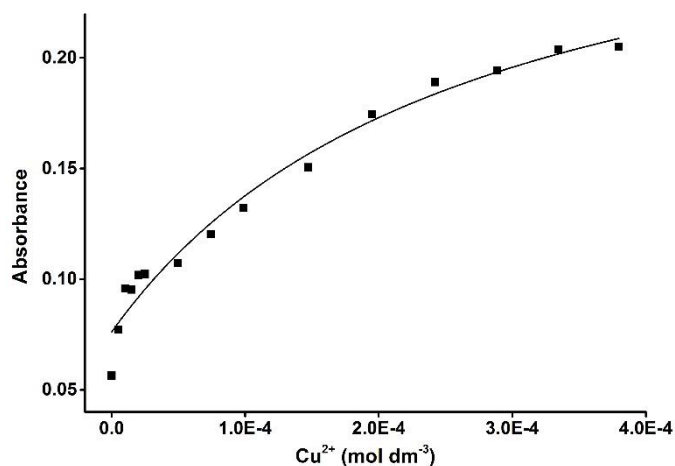


Figure S5. Absorbance at 555 nm of water (pH 7.4)-acetonitrile 90:10 v/v ($1.0 \times 10^{-5} \text{ mol L}^{-1}$) solutions of probe **1** upon addition of increasing quantities of Cu(II).

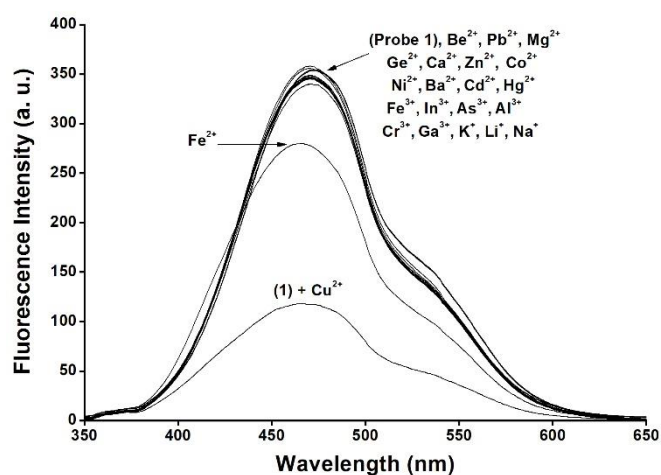


Figure S6. Fluorescence spectra (excitation at 320 nm) of probe **1** in water (pH 7.4)-acetonitrile 90:10 v/v ($1.0 \times 10^{-5} \text{ mol L}^{-1}$) upon addition of selected metal cations (10 eq.).

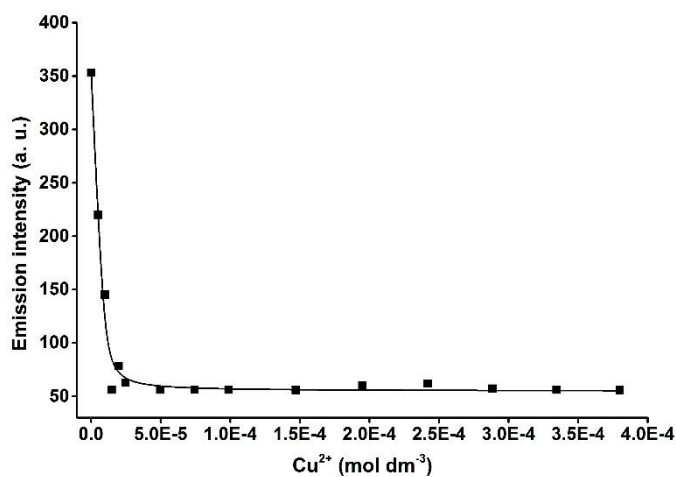


Figure S7. Fluorescence at 475 nm (excitation at 320 nm) of water (pH 7.4)-acetonitrile 90:10 v/v ($1.0 \times 10^{-5} \text{ mol L}^{-1}$) solutions of probe **1** upon addition of increasing quantities of Cu(II).

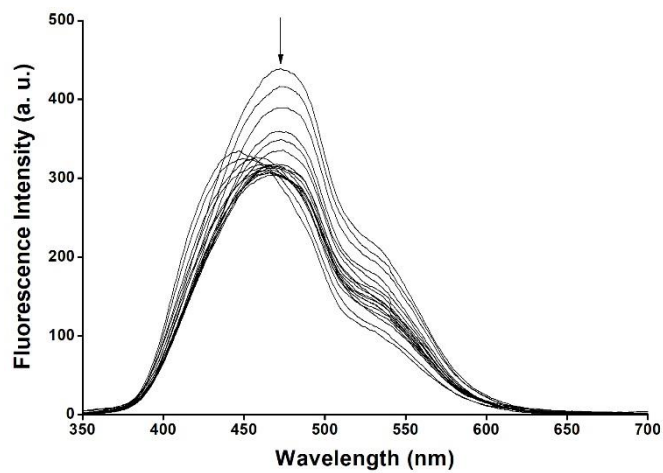


Figure S8. Emission spectra of probe **1** in water (pH 5.0)-acetonitrile 90:10 v/v ($1.0 \times 10^{-5} \text{ mol L}^{-1}$) solutions of probe **1** upon addition of increasing quantities of Cu(II).

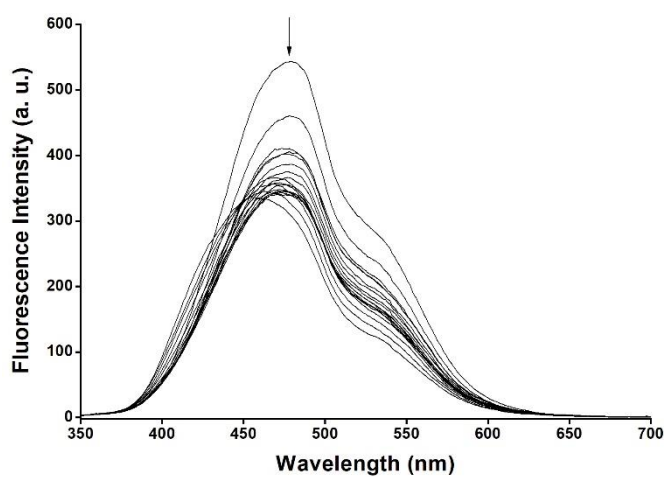


Figure S9. Emission spectra of probe **1** in water (pH 6.0)-acetonitrile 90:10 v/v ($1.0 \times 10^{-5} \text{ mol L}^{-1}$) solutions of probe **1** upon addition of increasing quantities of Cu(II).

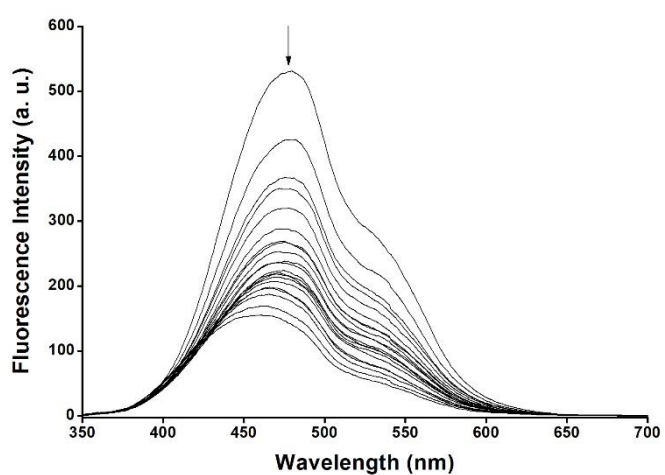


Figure S10. Emission spectra of probe **1** in water (pH 8.0)-acetonitrile 90:10 v/v ($1.0 \times 10^{-5} \text{ mol L}^{-1}$) solutions of probe **1** upon addition of increasing quantities of Cu(II).

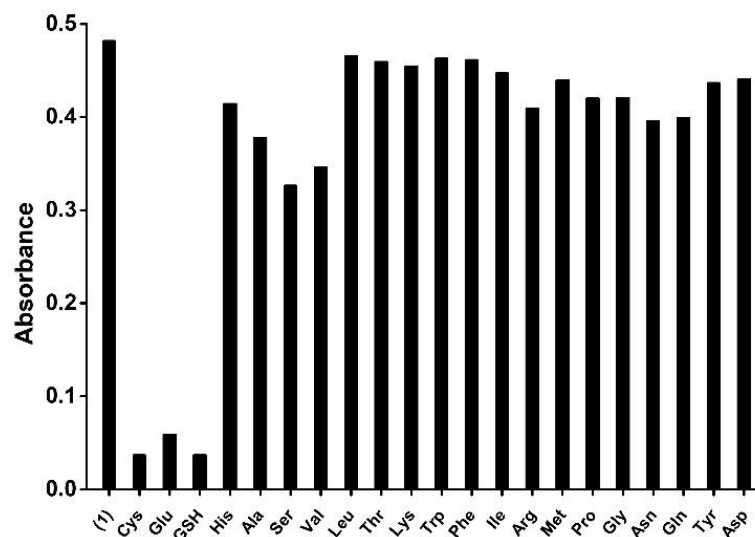


Figure S11. Absorbance at 555 nm of water (pH 7.4)-acetonitrile 90:10 v/v solutions of **1**-Cu(II) complex ($6.2 \times 10^{-6} \text{ mol L}^{-1}$) in the presence of Cys, Hcy and GSH (0.3 eq.) and selected amino acids (0.3 eq.).

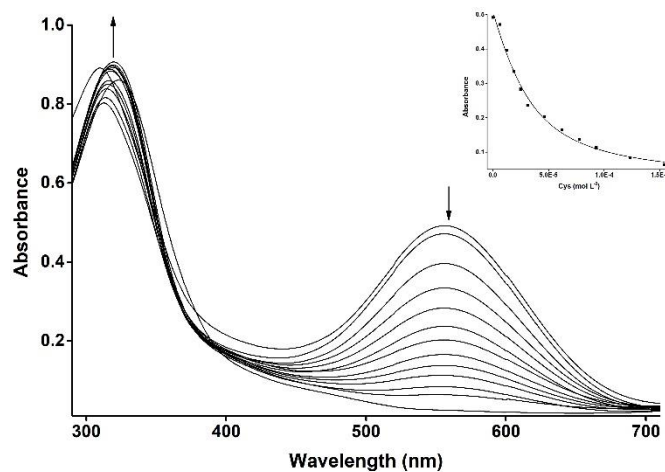


Figure S12. UV/Vis. titration profile of **1**-Cu(II) complex ($6.2 \times 10^{-6} \text{ mol L}^{-1}$) in water (pH 7.4)-acetonitrile 90:10 v/v upon addition of Cys (0 - 1.0 equivalents). Inset: Absorbance at 555 nm vs Cys concentration.

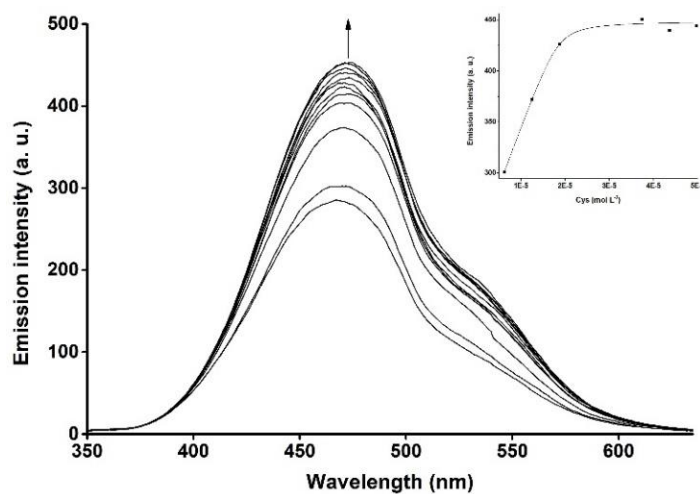


Figure S13. Fluorescence spectral changes of water (pH 7.4)-acetonitrile 90:10 v/v solutions of **1**-Cu(II) complex ($6.2 \times 10^{-6} \text{ mol L}^{-1}$) upon addition of increasing quantities of Cys (excitation at 324 nm). Inset emission at 475 nm vs. Cys concentration.

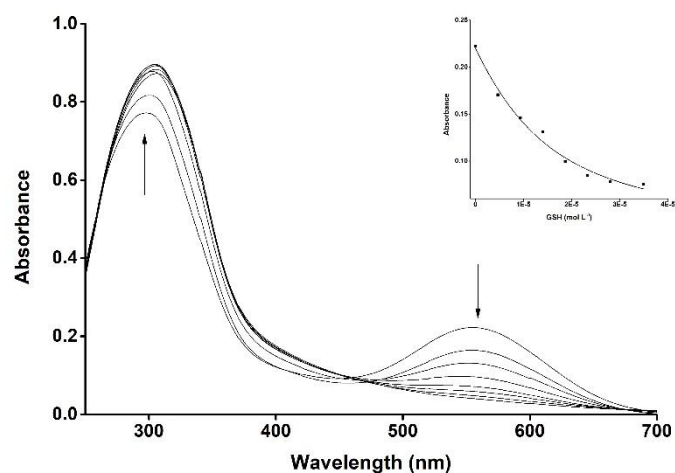


Figure S14. UV/Vis. titration profile of **1**-Cu(II) complex ($6.2 \times 10^{-6} \text{ mol L}^{-1}$) in water (pH 7.4)-acetonitrile 90:10 v/v upon addition of GSH (0 – 0.8 equivalents). Inset: Absorbance at 555 nm vs GSH concentration.

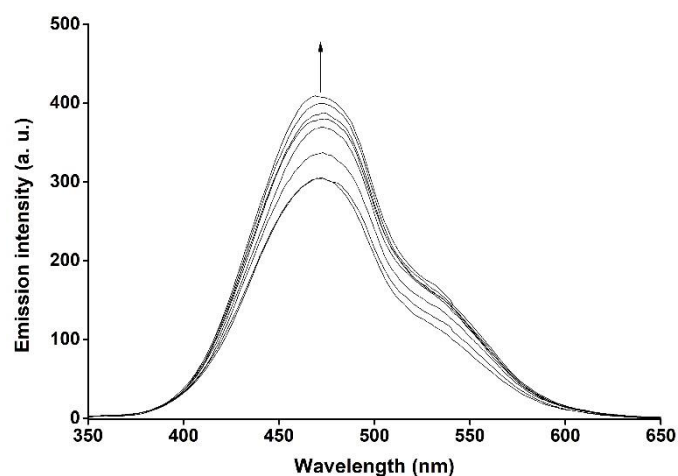


Figure S15. Fluorescence spectral changes of water (pH 7.4)-acetonitrile 90:10 v/v solutions of **1**-Cu(II) complex ($6.2 \times 10^{-6} \text{ mol L}^{-1}$) upon addition of increasing quantities of GSH (excitation at 324 nm).

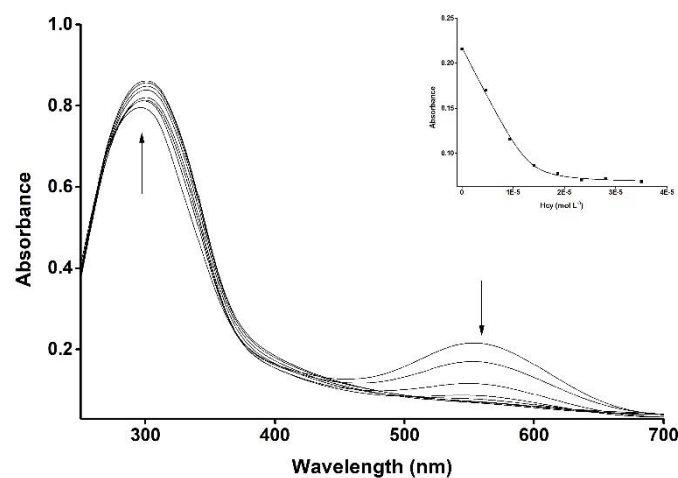


Figure S16. UV/Vis. titration profile of **1**-Cu(II) complex ($6.2 \times 10^{-6} \text{ mol L}^{-1}$) in water (pH 7.4)-acetonitrile 90:10 v/v upon addition of Hcy (0 – 0.8 equivalents). Inset: Absorbance at 555 nm vs Hcy concentration.

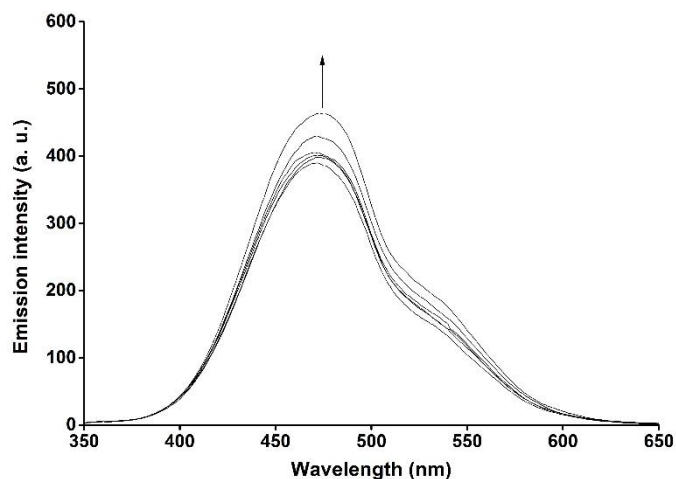


Figure S17. Fluorescence spectral changes of water (pH 7.4)-acetonitrile 90:10 v/v solutions of **1**-Cu(II) complex ($6.2 \times 10^{-6} \text{ mol L}^{-1}$) upon addition of increasing quantities of Hcy (excitation at 324 nm).

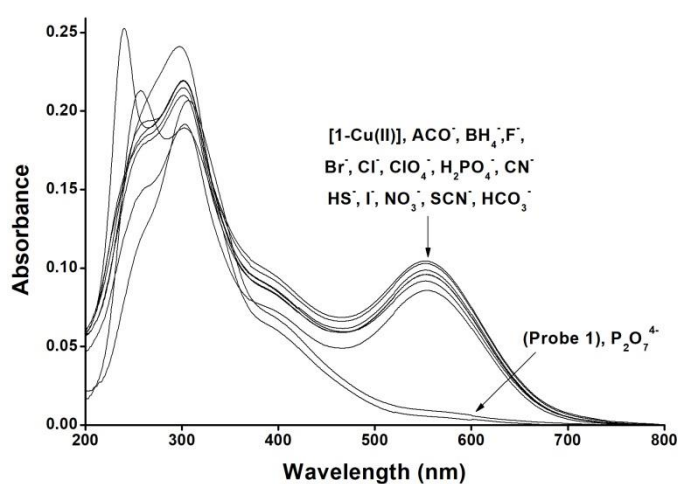


Figure S18. UV-visible changes of **1**-Cu(II) ($3.2 \times 10^{-6} \text{ mol L}^{-1}$) in water (pH 7.4)-acetonitrile 90:10 v/v in the presence of selected anions (0.2 eq.).

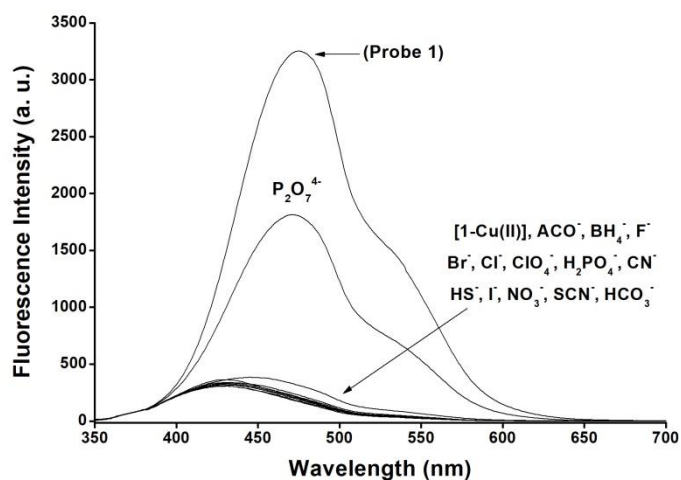


Figure S19. Changes in the emission band of **1**-Cu(II) complex ($3.2 \times 10^{-6} \text{ mol L}^{-1}$) in water (pH 7.4)-acetonitrile 90:10 v/v upon addition of selected anions (0.2 eq.).

Table S1. Analytical features of recently chromo-fluorogenic probes for biothiols detection recently published.

Probe	Mechanism	Media	Response	Limit of detection (μM)	Reference
Imidazole derivative-Cu(II) complex	Demetallation	Water-ACN 9:1	Cys, Hcy, GSH	6.5 (Cys); 5.0 (Hcy); 10.2 (GSH)	This paper
Fluorescein derivative-Cu(II) complex	Demetallation	Hepes	Cys, Hcy, GSH	0.12 (Cys); 0.036 (Hcy); 0.024 (GSH)	41
Naphthol derivative-Cu(II) complex	Demetallation	Water-DMSO 7:3	Cys (Hcy and GSH not tested)	2.9	42
Hydroxynaphthalene derivative-Cu(II) complex	Demetallation	Tris-DMSO 1:1	Cys	10.77	43
Anthracenyl derivative-Cu(II) complex	Demetallation	Hepes-ACN 3:7	Cys	0.019	44
Hydroxyjulolidine derivative-Cu(II) complex	Demetallation	Tris-DMF 5:1	Cys	3.6	45
Hydroxyjulolidine derivative-Cu(II) complex	Demetallation	Tris-DMSO 2:8	Cys	7.82	46
BODIPY derivative	Michael addition	Hepes-ACN 8:2	Cys	Not reported	28
Coumarin derivative	Michael addition	Water-MeOH 1:1	Cys, Hcy, GSH	0.192 (Cys); 0.158 (Hcy); 0.155 (GSH)	29
Triphenylamine derivative	Michael addition	Hepes-MeOH 1:1	Cys, Hcy, GSH	0.13 (Cys); 0.12 (Hcy); 0.085 (GSH)	30
Coumarin derivative-Cu(II) complex	Cu(II)/Cu(I) conversion	Hepes	Cys, Hcy, GSH	Not reported (Cys); not reported (Hcy); 15 (GSH)	31
Cyanine derivative	Aldehyde-thiazoline conversion	PBS	Cys, Hcy	0.008 (Cys); 0.008 (Hcy)	32
BODIPY derivative	Aldehyde-thiazoline conversion	Water-ACN 2:8	Cys, Hcy	Not reported (Cys); 2 (Hcy)	33
Binaphthyl derivative	Aldehyde-thiazoline conversion	Hepes-EtOH 2:98	Hcy	54	34
Pyronin derivative containing 4-methoxythiophenol	Nucleophilic aromatic substitution	PBS	Cys, Hcy, GSH	Not reported (Cys); not reported (Hcy); not reported (GSH)	35
Cyanine derivative containing 4-methoxythiophenol	Nucleophilic aromatic substitution	Hepes-DMSO 4:1	Cys	1.26	36
Fluorescein derivative	Hydrolysis of an acrylate ester	PBS-DMSO 7:3	Cys	0.084	37
Iminocoumarin derivative	Hydrolysis of a 2,4-dinitrobenzenesulfonyl moiety	PBS	Cys, Hcy, GSH	5.0 (Cys); 10.0 (Hcy); 5.0 (GSH)	38

Fluorescence quantum yield measurements

The fluorescence quantum yield of pyrene in cyclohexane ($\varphi_f = 0.32$) was used as a reference to measure the fluorescence quantum yields of probe **1** and complex [**1**-Cu(II)]. The following equation was used to calculate the fluorescence quantum yield:

$$\varphi_s = \varphi_f \frac{I_s A_f \eta_s^2}{I_f A_s \eta_r^2}$$

Here φ_f is the fluorescence quantum yield of reference. I stand for the integrated area under the emission curves. The subscripts s and r stand for sample and reference, respectively. A is the absorbance at a particular excitation wavelength. η is the refractive index of the medium. The absorbance of the dye at the excitation wavelength was always kept ~ 0.1 . The steady state absorption and emission spectra were fitted by the log normal line shape function. Consequently the fluorescence quantum yield for probe **1** is $\varphi = 0.26$ and for [**1**-Cu(II)] complex is $\varphi = 0.07$.